Chemical Science

EDGE ARTICLE

View Article Online
View Journal | View Issue

Cite this: *Chem. Sci.*, 2019, **10**, 3616

All publication charges for this article have been paid for by the Royal Society of Chemistry

Single-site metal–organic framework catalysts for the oxidative coupling of arenes *via* C–H/C–H activation†

Niels Van Velthoven,[a] Steve Waitschat,[b] Sachin M. Chavan,[cd] Pei Liu,[e] Simon Smolders,[a] Jannick Vercammen,[a] Bart Bueken,[a] Sara Bals,[e] Karl Petter Lillerud,[cd] Norbert Stock[bd] and Dirk E. De Vos*[a]

C–H activation reactions are generally associated with relatively low turnover numbers (TONs) and high catalyst concentrations due to a combination of low catalyst stability and activity, highlighting the need for recyclable heterogeneous catalysts with stable single-atom active sites. In this work, several palladium loaded metal–organic frameworks (MOFs) were tested as single-site catalysts for the oxidative coupling of arenes (*e.g.* *o*-xylene) *via* C–H/C–H activation. Isolation of the palladium active sites on the MOF supports reduced Pd(0) aggregate formation and thus catalyst deactivation, resulting in higher turnover numbers (TONs) compared to the homogeneous benchmark reaction. Notably, a threefold higher TON could be achieved for palladium loaded MOF-808 due to increased catalyst stability and the heterogeneous catalyst could efficiently be reused, resulting in a cumulative TON of 1218 after three runs. Additionally, the palladium single-atom active sites on MOF-808 were successfully identified by Fourier transform infrared (FTIR) and extended X-ray absorption fine structure (EXAFS) spectroscopy.

Received 10th December 2018
Accepted 17th February 2019

DOI: 10.1039/c8sc05510f

rsc.li/chemical-science

Introduction

The synthesis of biaryls has attracted much attention over the past decades since these motifs are abundantly present in pharmaceuticals, natural products, agrochemicals, specialty monomers and other fine chemicals.[1–4] Typically, the synthesis of the biaryl groups in these compounds involves conventional coupling reactions, such as the Suzuki reaction, which requires pre-functionalized substrates and produces stoichiometric amounts of salt waste.[1] In recent years, formation of biaryls *via* palladium catalyzed cross-dehydrogenative coupling (CDC) reactions has been proposed as a more cost-efficient and environmentally benign alternative, since simple arenes can be used as substrate and water is the only byproduct if O_2 is used as the oxidant.[5–7]

The primary focus of the scientific community regarding C–H activation of aromatic C(sp^2)–H bonds has been so far on increasing the catalysts' activity and regioselectivity, besides expanding the substrate scope.[8–13] However, given the relatively low turnover numbers (TONs) and high catalyst concentrations generally associated with CDC reactions compared to conventional coupling reactions, efficient recovery and recycling of the precious homogeneous palladium catalyst is a key aspect in the eventual implementation of this new synthetic strategy.[14] Moreover, since the valence state of palladium changes between Pd(II) and Pd(0) in the catalytic cycle, formation of Pd(0) aggregates is commonly recognized as an important deactivation pathway (Scheme 1), highlighting the need for solid catalysts with stable single-atom active sites.[15–17] Nevertheless, only very few heterogeneous catalysts for the oxidative coupling of arenes *via* C–H/C–H activation have been reported so far.[18–22]

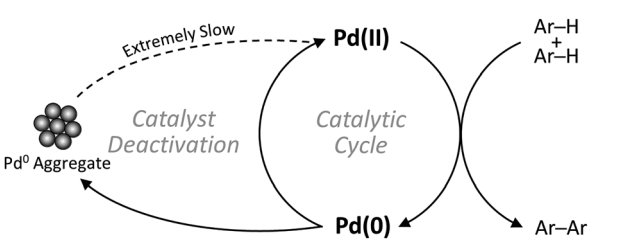

Scheme 1 Schematic representation of catalyst deactivation.

[a]*Centre for Surface Chemistry and Catalysis, KU Leuven, Celestijnenlaan 200F P. O. Box 2461, 3001 Leuven, Belgium. E-mail: dirk.devos@kuleuven.be*

[b]*Institute of Inorganic Chemistry, Christian-Albrechts University Kiel, Max-Eyth-Straße 2, 24118 Kiel, Germany*

[c]*Department of Chemistry, University of Oslo, P. O. Box 1033 Blindern, 0315 Oslo, Norway*

[d]*ProfMOF AS, Kirkegårdsveien 45, 3616 Kongsberg, Norway*

[e]*Electron Microscopy for Materials Science, University of Antwerp, Groenenborgerlaan 171, 2020 Antwerp, Belgium*

† Electronic supplementary information (ESI) available: Detailed experimental procedures, optimization of the reaction conditions, additional characterization data, substrate scope. See DOI: 10.1039/c8sc05510f

Metal–organic frameworks (MOFs), which are coordination polymers made up of inorganic secondary building units (SBUs; metal ions or clusters) and organic linkers, are an interesting group of porous, crystalline materials that can be transformed into heterogeneous single-site catalysts.[23–26] Besides any catalytic activity inherent to MOFs, common strategies to imbue MOFs with well-defined and isolated active sites include anchoring active transition metals on the organic linkers[27–31] or grafting them on open coordination sites of the SBUs.[31–40] Due to their excellent stability, combined with high surface areas and tunable porosity, Zr-based MOFs have already been proven to be interesting heterogeneous scaffolds to anchor metals for several applications ranging from sensing to catalysis.[41–45]

Herein, we present the first heterogeneous MOF-based catalysts for the oxidative coupling of arenes *via* C–H/C–H activation, which exhibit superior TONs compared to their homogeneous analogues due to isolation of the Pd(II) centers on the MOF supports.

Results and discussion

Screening of MOF supports

The oxidative homocoupling of *o*-xylene *via* C–H/C–H activation (Scheme 2) is considered to be a scientifically and industrially relevant CDC model reaction, since the 3,3′,4,4′-tetramethylbiphenyl product is an important intermediate in a more cost-efficient route to prepare the high-performance polyimide resin Upilex.[7,14,46] Industrially, the reaction is stopped at low conversion to avoid oligomerization of the products and the starting feedstock is recycled. This justifies evaluating the reaction using a TON value instead of a single-pass yield.[7] As a first step, several Zr-MOFs were evaluated for their potential as heterogeneous supports in the oxidative coupling of *o*-xylene (Table 1). Generally, an equimolar amount of MOF (based on its structural formula) with respect to $Pd(OAc)_2$ was added, *i.e.* one Zr_6-cluster of UiO-66 or MOF-808 per Pd atom. This ensures that a 4–6 fold excess of anchoring sites per Pd center are present in the frameworks (Table S1†). Additionally, 1-propanesulfonic acid was employed as strongly acidic additive, since recent findings by the group of Stahl reveal that strong acids or their corresponding salts dramatically increase the activity of Pd(II) for this reaction.[12] Inspired by the excellent results obtained with 2,2′-bipyridine-grafted mesoporous silica for the related Pd(II)-catalyzed oxidative Heck coupling,[17] a MOF containing 2,2′-bipyridine-5,5′-dicarboxylate ($bpydc^{2-}$) linkers (UiO-67-bipy; $[Zr_6(\mu_3\text{-}O)_4(\mu_3\text{-}OH)_4(bpydc)_6]$)[27] was tested. However, the addition of this MOF resulted in a dramatic decrease in activity *versus* the homogeneous reaction (Table 1; entry 1 and 2). A similar deactivation effect was found for the analogous dissolved heterocyclic nitrogen-containing ligand, 4,4′-dimethyl-2,2′-bipyridine (Table S2†). Consequently, other MOFs featuring anchoring sites which correspond more closely to the carboxylates in the active $Pd(OAc)_2$ complex were investigated. For instance, a UiO-66 analogue with pendent carboxylic acid groups as Pd(II) anchoring sites (UiO-66-COOH; $[Zr_6(\mu_3\text{-}O)_4(\mu_3\text{-}OH)_4(bdc\text{-}COOH)_6]$, bdc^{2-}-COOH = 1,2,4-benzenetricarboxylate)[47] was synthesized and tested. In contrast to UiO-67-bipy, a significantly higher TON than in the homogeneous case was obtained after the same reaction time (Table 1; entry 3), highlighting the positive effect of active site isolation by anchoring the active Pd(II) centers on the pendent carboxylic acid groups. Inspired by previous research in which platinum-group metal complexes were grafted onto the inorganic SBUs of a MOF support,[35,38,40] several Zr-MOFs with available coordination sites on the clusters (hydrogen-bonded OH/OH_2 pairs)[39] were synthesized (MOF-808, UMCM-309a and Zr-abtc). The hexanuclear Zr-clusters of MOF-808 ($[Zr_6(\mu_3\text{-}O)_4(\mu_3\text{-}OH)_4(btc)_2(CH_3COO)_6]$, btc^{3-} = 1,3,5-benzenetricarboxylate)[48,49] are 6-fold coordinated by btc^{3-} linkers, resulting in up to 6 open sites per cluster, after removing the acetate modulators using a simple acid treatment. A closely related MOF with 6-fold coordinated Zr-clusters is UMCM-309a ($[Zr_6(\mu_3\text{-}O)_4(\mu_3\text{-}OH)_4(btb)_2(HCOO)_6]$, btb^{3-} = 1,3,5-(4-carboxylphenyl) benzene),[50] which features a stable two-dimensional layered network instead of a three-dimensional framework. Recently, a new 8-connected Zr-MOF with 3,3′,5,5′-azobenzene-tetracarboxylate ($abtc^{4-}$) linkers ($[Zr_6(\mu_3\text{-}O)_4(\mu_3\text{-}OH)_4(abtc)_2(OH)_4(\text{-}H_2O)_4]$) was reported,[51] which contains 4 open sites per cluster and could be synthesized following a newly developed water-based green synthesis procedure (Fig. S2†). In line with the increase in activity for UiO-66-COOH, the addition of MOFs with open sites on the Zr-clusters resulted in significantly higher TONs compared to the homogeneous reference case (Table 1; entries 4–6). In addition, UiO-66 ($[Zr_6(\mu_3\text{-}O)_4(\mu_3\text{-}OH)_4(bdc)_6]$, bdc^{2-} = 1,4-benzenedicarboxylate),[52] a well-known non-functionalized Zr-MOF, was tested as a reference, since it does not contain significant amounts of pendent carboxylic acid groups or open sites on the Zr-clusters to which Pd(II) could coordinate. The TON observed in the presence of UiO-66 was similar to that observed for homogeneous $Pd(OAc)_2$ (Table 1; entry 7). This confirms that the increase in TON observed for other MOFs like MOF-808 is due to active site isolation of the Pd on the anchoring sites of the MOFs. Besides MOFs with anchoring sites, a moderate increase in TON could also be achieved by the addition of high-surface area zirconium oxide. Finally, higher chemoselectivities were obtained in the presence of MOFs with open sites on the Zr-clusters or pendent carboxylic acid groups since less triaryl side products were formed. The formation of these bulky triaryls may be suppressed in the presence of MOFs due to pore confinement.

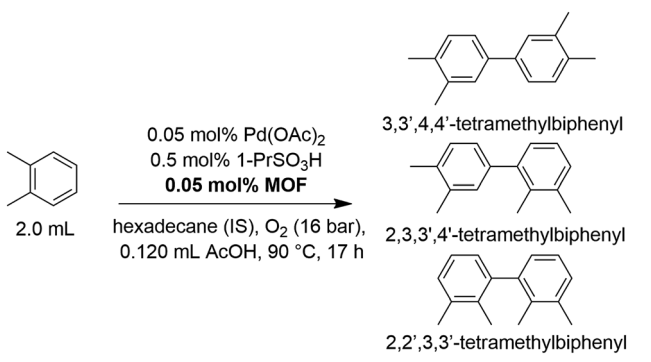

Scheme 2 The oxidative coupling of *o*-xylene under the standard reaction conditions: *o*-xylene (16.58 mmol), $Pd(OAc)_2$ (8.29 μmol), MOF support (8.29 μmol), 1-propanesulfonic acid (82.85 μmol), acetic acid co-solvent (2.07 mmol), 90 °C, 16 bar O_2, 17 h.

Table 1 Screening of the different MOF supports under the standard reaction conditions (cfr. Scheme 2)

Entry	MOF support	Chemo-selectivity[a] (%)	Regio-selectivity[b] (%)	Yield[c] (%)	TON[d]	TOF[e] (h^{-1})
1	—	88	71	4.9	97	8.1
2	UiO-67-bipy	74	66	0.3	6	1.1
3	UiO-66-COOH	92	73	7.4	149	10.6
4	MOF-808	92	74	9.2	183	11.2
5	UMCM-309a	93	74	8.4	168	11.1
6	Zr-abtc	93	73	7.1	142	11.0
7	UiO-66	90	75	5.1	103	8.3
8	ZrO_2[f]	89	75	6.5	130	10.5

[a] Chemoselectivity is defined as the percentage of biaryls relative to all formed products (oxidation products, biaryls and triaryls). [b] Regioselectivity is defined as the percentage of 3,3′,4,4′-tetramethylbiphenyl relative to all three biaryls. [c] Yield was determined by GC-FID with hexadecane as internal standard. [d] TON is defined as TON = 2 × mole (biaryl)/mole (Pd). [e] TOF was determined after 4 h. [f] 10 mg of zirconium oxide was added.

Heterogeneity of the single-site MOF catalysts

The heterogeneity of the single-site MOF catalysts was studied by recycling tests and metals analysis of the reaction solution. After the reaction, the sample was centrifuged and the MOF crystals were separated from the reaction solution. Fresh reactant (*e.g.* *o*-xylene), co-solvent (*e.g.* acetic acid), internal standard and strongly acidic additive (*e.g.* 1-propanesulfonic acid) were added to the recycled MOF and the reaction was resumed for a second run. Materials with open sites on the Zr-clusters (MOF-808, UMCM-309a and Zr-abtc) retained their activity better than UiO-66-COOH with pendent carboxylic acid groups, resulting in higher cumulative TONs after 4 runs (Fig. 1). In line with these results, a lower cumulative TON was noticed for UiO-66, which does not contain anchoring sites. In addition, the palladium and zirconium contents of the reaction solution were measured after the first run by inductively coupled plasma optical emission spectrometry (ICP-OES) (Table S3†). Generally, palladium leaching could be minimized to approximately 5% for MOFs with open sites on the Zr-cluster (MOF-808 and Zr-abtc) and no significant zirconium leaching was detected. However, more leaching was observed for UMCM-309a, presumably due to its two-dimensional layered structure. Higher leaching values were also obtained for UiO-66-COOH and UiO-66, indicating that palladium is best retained on MOFs with open sites on the Zr-clusters and with a three-dimensional pore structure, like MOF-808. Furthermore, an acrylic acid grafted polyolefin fiber (Smopex-102), one of the very few already reported heterogeneous supports for the oxidative coupling of arenes,[22] was tested using a similar ratio of 1 Pd(II) center per 6 pendent carboxylic acid groups. The cumulative TON of this Pd-loaded polymer with pendent carboxylic acid groups is substantially lower than the TON of its MOF analogue (UiO-66-COOH), which might be due to inferior accessibility of the carboxylic acid groups. In addition, the stability of the MOFs was evaluated by comparing the powder X-ray diffraction patterns before and after the reaction (Fig. S5–S10†). No significant decrease in crystallinity was observed for MOF-808, UMCM-309a, Zr-abtc, UiO-66-COOH and UiO-66 after four runs at 90 °C. In contrast, UiO-67-bipy largely lost its long-range order after exposure to the reaction solvent and conditions.

Substrate scope

In view of its superior activity, heterogeneity and facile synthesis procedure, MOF-808 was selected as model support to expand the substrate scope (Fig. S11†). High TONs were obtained for the homocoupling of toluene and *tert*-butylbenzene, while the

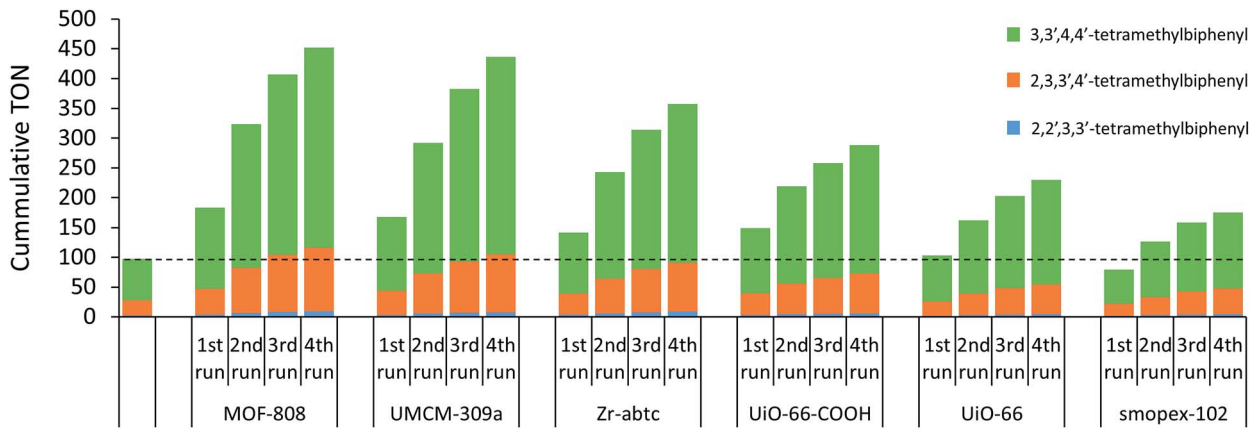

Fig. 1 Recycling experiments of several heterogeneous supports for the Pd-catalyzed oxidative coupling of *o*-xylene performed under the standard reaction conditions.

activity was significantly lower for the coupling of *p*-xylene and 1,2-difluorobenzene due to steric hindrance and electron-withdrawing effects, respectively.

Optimizing the reaction conditions

Significantly higher TONs for the oxidative coupling of *o*-xylene could be obtained for the heterogeneous system with MOF-808 by increasing the reaction temperature (Fig. 2). Notably, at 110 °C, the TON is 2.9 times higher for the MOF-808 system than for the analogous homogeneous system, which is a clear benefit of active site isolation enabled by the MOF. At even higher temperatures, the MOF support started to decompose (Fig. S12†), resulting in lower TONs, which were more comparable to those of the homogeneous system. After further optimizing the palladium loading of the MOF and the amount of 1-propanesulfonic acid and co-solvent (Table S2†), a TON of 436 ± 17 could be reached after the first run (Fig. 3) with only 2% Pd leaching (Table S4†). Since oxygen is used as terminal oxidant, a stoichiometric amount of water is produced and partially absorbed by the hydrophilic MOF material. Product inhibition experiments revealed that the formation of water did not lead to a significant decrease in activity at short reaction times (Fig. S13†). However, after many catalytic cycles (TONs > 400), a large amount of water is formed and product inhibition due to water formation is observed (Table S2†). Nevertheless, the activity of the solid MOF-based catalyst could be restored by reactivating the MOF materials after each run under vacuum (1 mbar) at room temperature for 24 h (Fig. 3). A cumulative TON of 1218 ± 36 with an overall regioselectivity of 73% for 3,3′,4,4′-tetramethylbiphenyl was obtained after three runs, which is well beyond the state-of-the-art.[12,22] Moreover, only 5% of Pd was leached after three runs (Table S4†).

Active site isolation

The binding mode of Pd(II) to the zirconium clusters of MOF-808 was studied by Fourier transform infrared spectroscopy (FTIR). Upon removal of a capping acetate from the cluster, a hydrogen-bonded OH/OH_2 pair occupies the place of the missing carboxylate. This OH/OH_2 pair displays a characteristic IR band at 2744 cm^{-1}, while the sharp IR band at 3672 cm^{-1} results from a combination of non-hydrogen-bonded OH groups and μ_3-OH groups inside the cluster (Fig. S15†).[53,54] In agreement with previous research,[33,35,36,38,55] the characteristic IR band at 2744 cm^{-1} disappears after chemisorption of the transition metal complex and the sharp IR band at 3672 cm^{-1} broadens, indicating that the palladium species interact with these open sites on the Zr-clusters. Moreover, the local environment of the MOF-supported Pd(II) was studied by X-ray absorption spectroscopy (XAS). In line with the FTIR data, the fit between the experimental and simulated extended X-ray absorption fine structure (EXAFS) data is excellent for the structure in which Pd(II) is anchored on the open site of the Zr-cluster after exchanging with the proton of the –OH_2 group and liberating acetic acid (Fig. 4). Furthermore, the absence of a clear peak around 2.6 Å confirms that the trimeric $Pd(OAc)_2$ complexes are converted into monomeric, MOF-supported Pd(II) species (Fig. S16†).[17,22] Hence, the Pd(II) species formed after the reoxidation step and possibly also the Pd(II) complex formed after the first C–H activation step, can be anchored on the MOF support (Scheme 3). High-angle annular dark-field scanning transmission electron microscopy (HAADF-STEM) images of MOF-808 and UiO-66 after reaction in combination with energy-dispersive X-ray spectroscopy (EDX) showed that palladium anchoring reduces Pd nanoparticle aggregation and thus deactivation after the reductive elimination step (Fig. S19–S22†).

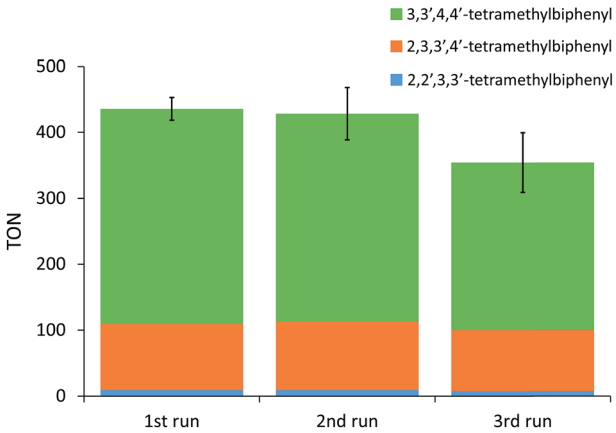

Fig. 3 Oxidative coupling of *o*-xylene performed under optimized reaction conditions and with reactivation of the Pd loaded MOF support under vacuum (1 mbar) at room temperature for 24 h in between consecutive runs. Conditions: *o*-xylene (16.58 mmol), $Pd(OAc)_2$ (8.29 μmol), MOF-808 (41.43 μmol), 1-propanesulfonic acid (331.40 μmol), acetic acid (2.07 mmol), 110 °C, 20 bar O_2, 17 h. The TONs are the average of three experiments.

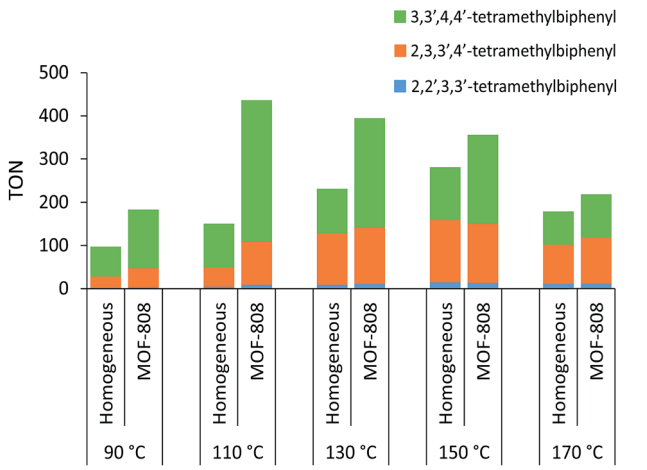

Fig. 2 Effect of temperature on the TON of the oxidative coupling of *o*-xylene with and without MOF-808 performed under the standard reaction conditions.

Reaction mechanism

Catalyst deactivation was studied by analyzing the reaction kinetics (Fig. 5). Although the homogeneous system was found

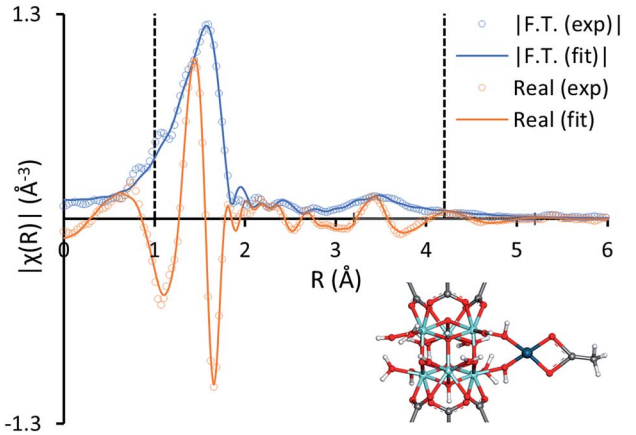

Fig. 4 The magnitude (blue) and real component (orange) of the Fourier transform of the experimental k^2-weighted Pd K-edge EXAFS spectra of preloaded MOF-808 (1 Pd per Zr-cluster in *o*-xylene) (hollow circles) and the corresponding fits of the structure model (solid lines) in *R*-space. The vertical dashed lines indicate the fitting range. The Zr, O, C, H and Pd atoms are represented in the structure model by turquoise, red, gray, white and dark blue spheres, respectively.

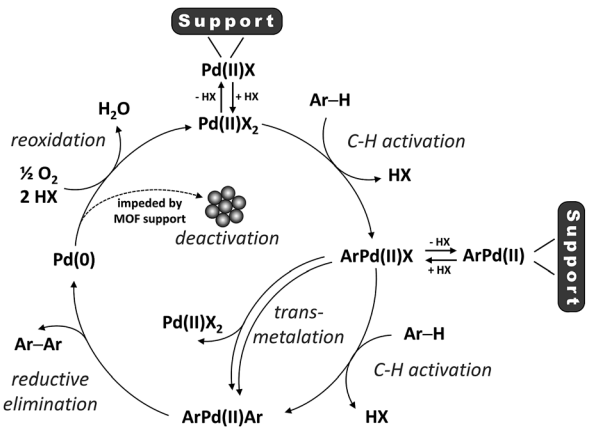

Scheme 3 The proposed catalytic cycle (X = acetate or 1-propanesulfonate).

to be the most active at short reaction times, only moderate yields were obtained at longer reaction times due to catalyst deactivation. On the contrary, almost no deactivation was observed when MOF-808 was added, with an essentially constant rate up to 24 h reaction time. This implies that catalyst lifetime can be considerably prolonged by isolating the active sites on the MOF material. Moreover, a maximum TON was achieved for the heterogeneous system if more than 8 bar O_2 was applied, indicating that deactivation is negligible under these conditions. In contrast, a clear dependence of the TON on the oxygen pressure could be seen in the homogeneous system for a wide range of oxygen pressures (Fig. S23†). To gather further insights into the catalytic mechanism, the kinetic isotope effect (KIE) was evaluated by comparing the conversion of *o*-xylene with *o*-xylene-d_{10} at short reaction times. The measured k_H/k_D values were 1.4 and 1.3 for the homogeneous

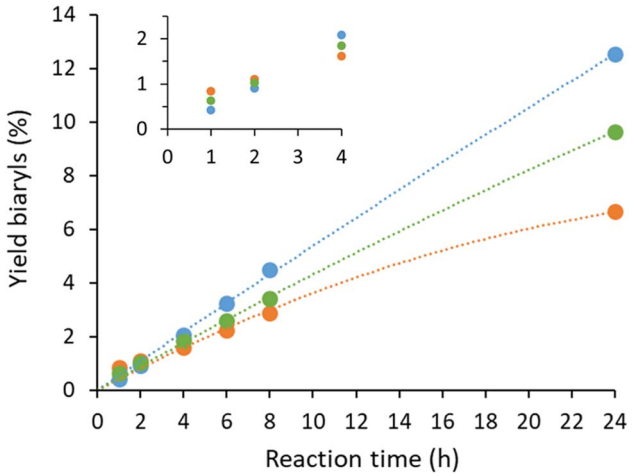

Fig. 5 Kinetic profiles of the oxidative coupling of *o*-xylene performed under the standard reaction conditions with MOF-808 (blue), UiO-66-COOH (green) and the homogeneous reaction without MOF support (orange). Lines were added as a guide to the eye.

and heterogeneous case, respectively, indicating a similar rate-limiting step for both systems. These modest KIE values are in accordance to the literature for the oxidative coupling of *o*-xylene under neat conditions.[14]

Conclusions

In this work, we have shown for the first time that palladium loaded Zr-MOFs can be efficient single-site solid hybrid catalysts for the oxidative coupling of arenes *via* C–H/C–H activation. MOFs with various anchoring sites were screened first and the heterogeneity of these solid catalysts was studied by recycling tests and metals analysis of the reaction solution, which indicated that the heterogeneous catalysts could efficiently be reused. After optimization of the reaction conditions, a three-fold higher TON could be achieved for the MOF-808 system compared to the analogous homogeneous system and Pd leaching was minimized to 2%. The activity of the solid MOF-based catalyst could be retained by reactivating the MOF materials by drying in between consecutive runs, resulting in a cumulative TON of 1218 after three runs. Finally, analysis of the reaction kinetics revealed that the superior TONs result from isolation of the active sites on the MOF material, which prolongs catalyst lifetime, and the isolated palladium single-atom active sites on MOF-808 were successfully identified by FTIR and EXAFS spectroscopy. These results show that the TON of palladium in C–H activation reactions can be significantly increased by developing stable heterogeneous single-site catalysts.

Conflicts of interest

There are no conflicts to declare.

Acknowledgements

The research leading to these results has received funding from the NMBP-01-2016 Program of the European Union's Horizon 2020 Framework Program H2020/2014-2020/under grant agreement no. [720996]. N. V. V., S. S., J. V., B. B. and D. E. D. V. thank the FWO for funding (SB, Aspirant and postdoctoral grants). The electron microscopy work was supported by FWO funding G038116. D. E. D. V. is grateful for KU Leuven support in the frame of the CASAS Metusalem project and a C3 type project. The XAS experiments were performed on beamline BM26A at the European Synchrotron Radiation Facility (ESRF), Grenoble, France. We are grateful to D. Banerjee at the ESRF for providing assistance in using beamline BM26A. Johnson Matthey and S. Bennett are gratefully acknowledged for providing Smopex-102.

Notes and references

1 T. J. Colacot and J. Matthey, *Platinum Met. Rev.*, 2011, **55**, 84–90.
2 C. S. Yeung and V. M. Dong, *Chem. Rev.*, 2011, **111**, 1215–1292.
3 Y. Yang, J. Lan and J. You, *Chem. Rev.*, 2017, **117**, 8787–8863.
4 C. Torborg and M. Beller, *Adv. Synth. Catal.*, 2009, **351**, 3027–3043.
5 D. C. Blakemore, L. Castro, I. Churcher, D. C. Rees, A. W. Thomas, D. M. Wilson and A. Wood, *Nat. Chem.*, 2018, **10**, 383–394.
6 Y. Wu, J. Wang, F. Mao and F. Y. Kwong, *Chem.–Asian J.*, 2014, **9**, 26–47.
7 Y. Izawa and S. S. Stahl, *Adv. Synth. Catal.*, 2010, **352**, 3223–3229.
8 T. W. Lyons, K. L. Hull and M. S. Sanford, *J. Am. Chem. Soc.*, 2011, **133**, 4455–4464.
9 N. Kuhl, M. N. Hopkinson, J. Wencel-Delord and F. Glorius, *Angew. Chem., Int. Ed.*, 2012, **51**, 10236–10254.
10 K. M. Engle, D. Wang and J. Yu, *J. Am. Chem. Soc.*, 2010, **132**, 14137–14151.
11 P. Wang, P. Verma, G. Xia, J. Shi, J. X. Qiao, S. Tao, P. T. W. Cheng, M. A. Poss, M. E. Farmer, K. S. Yeung and J. Q. Yu, *Nature*, 2017, **551**, 489–493.
12 D. Wang and S. S. Stahl, *J. Am. Chem. Soc.*, 2017, **139**, 5704–5707.
13 B. J. Gorsline, L. Wang, P. Ren and B. P. Carrow, *J. Am. Chem. Soc.*, 2017, **139**, 9605–9614.
14 C. A. M. R. Van Slagmaat, G. K. M. Verzijl, L. Lefort, P. L. Alsters and M. Fern, *ChemCatChem*, 2018, **10**, 2620–2626.
15 E. M. Ferreira, H. Zhang and B. M. Stoltz, *Tetrahedron*, 2008, **64**, 5987–6001.
16 Y. Liu, X. Wang, X. Cai, G. Chen, J. Li, Y. Zhou and J. Wang, *ChemCatChem*, 2016, **8**, 448–454.
17 H. Duan, M. Li, G. Zhang, J. R. Gallagher, Z. Huang, Y. Sun, Z. Luo, H. Chen, J. T. Miller, R. Zou, A. Lei, Y. Zhao, T. Miller, R. Zou, A. Lei, Y. Zhao, J. T. Miller, R. Zou, A. Lei and Y. Zhao, *ACS Catal.*, 2015, **5**, 3752–3759.
18 T. Ishida, S. Aikawa, Y. Mise, R. Akebi, A. Hamasaki, T. Honma, H. Ohashi, T. Tsuji, Y. Yamamoto, M. Miyasaka, T. Yokoyama and M. Tokunaga, *ChemSusChem*, 2015, **8**, 695–701.
19 T. Ishida, R. Tsunoda, Z. Zhang, A. Hamasaki, T. Honma, H. Ohashi, T. Yokoyama and M. Tokunaga, *Appl. Catal., B*, 2014, **150**, 523–531.
20 G. Mitran, O. D. Pavel, M. Florea and V. I. Pârvulescu, *Appl. Catal., A*, 2016, **514**, 71–82.
21 L. M. Neal and H. E. Hagelin-Weaver, *J. Mol. Catal. A: Chem.*, 2008, **284**, 141–148.
22 Y. Liu, Y. Zhou, J. Li, Q. Wang, Q. Qin, W. Zhang, H. Asakura, N. Yan and J. Wang, *Appl. Catal., B*, 2017, **209**, 679–688.
23 H. Furukawa, K. E. Cordova, M. O'Keeffe and O. M. Yaghi, *Science*, 2013, **341**, 1230444.
24 H. C. Zhou, J. R. Long and O. M. Yaghi, *Chem. Rev.*, 2012, **112**, 673–674.
25 A. Corma, H. García and F. X. Llabrés i Xamena, *Chem. Rev.*, 2010, **110**, 4606–4655.
26 J. Gascon, A. Corma, F. Kapteijn and F. X. Llabrés I Xamena, *ACS Catal.*, 2014, **4**, 361–378.
27 S. Øien, G. Agostini, S. Svelle, E. Borfecchia, K. A. Lomachenko, L. Mino, E. Gallo, S. Bordiga, U. Olsbye, K. P. Lillerud and C. Lamberti, *Chem. Mater.*, 2015, **27**, 1042–1056.
28 X. Li, R. Van Zeeland, R. V. Maligal-Ganesh, Y. Pei, G. Power, L. Stanley and W. Huang, *ACS Catal.*, 2016, **6**, 6324–6328.
29 R. Van Zeeland, X. Li, W. Huang and L. M. Stanley, *RSC Adv.*, 2016, **6**, 56330–56334.
30 L. Chen, S. Rangan, J. Li, H. Jiang and Y. Li, *Green Chem.*, 2014, **16**, 3978–3985.
31 S. M. J. Rogge, A. Bavykina, J. Hajek, H. Garcia, A. I. Olivos-Suarez, A. Sepúlveda-Escribano, A. Vimont, G. Clet, P. Bazin, F. Kapteijn, M. Daturi, E. V. Ramos-Fernandez, F. X. I. Llabrés Xamena, V. Van Speybroeck and J. Gascon, *Chem. Soc. Rev.*, 2017, **46**, 3134–3184.
32 R. J. Drout, A. J. Howarth, K. Otake, T. Islamoglu and O. K. Farha, *CrystEngComm*, 2018, **20**, 6140–6145.
33 K. Otake, Y. Cui, C. T. Buru, Z. Li, J. T. Hupp and O. K. Farha, *J. Am. Chem. Soc.*, 2018, **140**, 8652–8656.
34 Z. Li, A. W. Peters, V. Bernales, M. A. Ortuño, N. M. Schweitzer, M. R. Destefano, L. C. Gallington, A. E. Platero-Prats, K. W. Chapman, C. J. Cramer, L. Gagliardi, J. T. Hupp and O. K. Farha, *ACS Cent. Sci.*, 2017, **3**, 31–38.
35 V. Bernales, D. Yang, J. Yu, G. Gümüşlu, C. J. Cramer, B. C. Gates and L. Gagliardi, *ACS Appl. Mater. Interfaces*, 2017, **9**, 33511–33520.
36 Z. Li, N. M. Schweitzer, A. B. League, V. Bernales, A. W. Peters, A. B. Getsoian, T. C. Wang, J. T. Miller, A. Vjunov, J. L. Fulton, J. A. Lercher, C. J. Cramer, L. Gagliardi, J. T. Hupp and O. K. Farha, *J. Am. Chem. Soc.*, 2016, **138**, 1977–1982.
37 K. Manna, P. Ji, Z. Lin, F. X. Greene, A. Urban, N. C. Thacker and W. Lin, *Nat. Commun.*, 2016, **7**, 1–11.

38 D. Yang, S. O. Odoh, J. Borycz, T. C. Wang, O. K. Farha, J. T. Hupp, C. J. Cramer, L. Gagliardi and B. C. Gates, *ACS Catal.*, 2016, **6**, 235–247.
39 T. F. Liu, N. A. Vermeulen, A. J. Howarth, P. Li, A. A. Sarjeant, J. T. Hupp and O. K. Farha, *Eur. J. Inorg. Chem.*, 2016, 4349–4352.
40 D. Yang, S. O. Odoh, T. C. Wang, O. K. Farha, J. T. Hupp, C. J. Cramer, L. Gagliardi and B. C. Gates, *J. Am. Chem. Soc.*, 2015, **137**, 7391–7396.
41 Y. Bai, Y. Dou, L.-H. Xie, W. Rutledge, J.-R. Li and H.-C. Zhou, *Chem. Soc. Rev.*, 2016, **45**, 2327–2367.
42 M. Zhao, S. Ou and C. De Wu, *Acc. Chem. Res.*, 2014, **47**, 1199–1207.
43 I. Nath, J. Chakraborty and F. Verpoort, *Chem. Soc. Rev.*, 2016, **45**, 4127–4170.
44 S. Yuan, J. S. Qin, C. T. Lollar and H. C. Zhou, *ACS Cent. Sci.*, 2018, **4**, 440–450.
45 J. S. Qin, S. Yuan, C. Lollar, J. Pang, A. Alsalme and H. C. Zhou, *Chem. Commun.*, 2018, **54**, 4231–4249.
46 N. Erdmann, Y. Su, B. Bosmans, V. Hessel and T. Noël, *Org. Process Res. Dev.*, 2016, **20**, 831–835.
47 F. Ragon, B. Campo, Q. Yang, C. Martineau, A. D. Wiersum, A. Lago, V. Guillerm, C. Hemsley, J. F. Eubank, M. Vishnuvarthan, F. Taulelle, P. Horcajada, A. Vimont, P. L. Llewellyn, M. Daturi, S. Devautour-Vinot, G. Maurin, C. Serre, T. Devic and G. Clet, *J. Mater. Chem. A*, 2015, **3**, 3294–3309.
48 H. Furukawa, F. Gándara, Y.-B. Zhang, J. Jiang, W. L. Queen, M. R. Hudson and O. M. Yaghi, *J. Am. Chem. Soc.*, 2014, **136**, 4369–4381.
49 W. Liang, H. Chevreau, F. Ragon, P. D. Southon, V. K. Peterson and D. M. D'Alessandro, *CrystEngComm*, 2014, **16**, 6530–6533.
50 J. Ma, A. G. Wong-Foy and A. J. Matzger, *Inorg. Chem.*, 2015, **54**, 4591–4593.
51 H. Wang, X. Dong, J. Lin, S. J. Teat, S. Jensen, J. Cure, E. V. Alexandrov, Q. Xia, K. Tan, Q. Wang, D. H. Olson, D. M. Proserpio, Y. J. Chabal, T. Thonhauser, J. Sun, Y. Han and J. Li, *Nat. Commun.*, 2018, **9**, 1–11.
52 J. H. Cavka, S. Jakobsen, U. Olsbye, N. Guillou, C. Lamberti, S. Bordiga and K. P. Lillerud, *J. Am. Chem. Soc.*, 2008, **6**, 13850–13851.
53 N. Planas, J. E. Mondloch, S. Tussupbayev, J. Borycz, L. Gagliardi, J. T. Hupp, O. K. Farha and C. J. Cramer, *J. Phys. Chem. Lett.*, 2014, **5**, 3716–3723.
54 D. Yang, V. Bernales, T. Islamoglu, O. K. Farha, J. T. Hupp, C. J. Cramer, L. Gagliardi and B. C. Gates, *J. Am. Chem. Soc.*, 2016, **138**, 15189–15196.
55 I. S. Kim, J. Borycz, A. E. Platero-Prats, S. Tussupbayev, T. C. Wang, O. K. Farha, J. T. Hupp, L. Gagliardi, K. W. Chapman, C. J. Cramer and A. B. F. Martinson, *Chem. Mater.*, 2015, **27**, 4772–4778.